

ChemComm

Accepted Manuscript



This article can be cited before page numbers have been issued, to do this please use: M. Li, J. Liu, T. Liu, M. Zhang and F. Pan, *Chem. Commun.*, 2018, DOI: 10.1039/C7CC08505B.



This is an Accepted Manuscript, which has been through the Royal Society of Chemistry peer review process and has been accepted for publication.

Accepted Manuscripts are published online shortly after acceptance, before technical editing, formatting and proof reading. Using this free service, authors can make their results available to the community, in citable form, before we publish the edited article. We will replace this Accepted Manuscript with the edited and formatted Advance Article as soon as it is available.

You can find more information about Accepted Manuscripts in the [author guidelines](#).

Please note that technical editing may introduce minor changes to the text and/or graphics, which may alter content. The journal's standard [Terms & Conditions](#) and the ethical guidelines, outlined in our [author and reviewer resource centre](#), still apply. In no event shall the Royal Society of Chemistry be held responsible for any errors or omissions in this Accepted Manuscript or any consequences arising from the use of any information it contains.



A versatile single molecular precursor for the synthesis of layered oxide cathode materials for Li-ion batteries

Maofan Li, Jiajie Liu, Tongchao Liu, Mingjian Zhang,* Feng Pan*

Received 00th January 2017,
Accepted 00th January 2017

DOI: 10.1039/x0xx00000x

www.rsc.org/

A carbonyl-bridged single molecular precursor LiTM(acac)₃ (TM = Ni/Co/Mn, acac=acetylacetonate) featured 1D chain structure, was designed and applied to achieve the layered oxide cathode materials LiTMO₂ (TM=Ni/Co/Mn, NMC) here. As representatives, layered oxides, primary LiCoO₂, binary LiNi_{0.8}Co_{0.2}O₂ and ternary LiNi_{0.5}Mn_{0.3}Co_{0.2}O₂ were successfully prepared as the cathode materials. When they are applied to Li-ion batteries (LIBs), all exhibit good electrochemical performance due to unique morphology and great uniformity of element distribution. This versatile precursor is predicted to accommodate many other metal cations, such as Na⁺, Al³⁺, Fe²⁺, due to the flexibility of organic ligand, which not only facilitates the doping-modification of NMC system, but also enables synthesizing Na-ion layered oxides. It opens a new avenue to synthesize high-performance layered oxide cathode materials for LIBs.

Layered oxides cathode materials, including LiCoO₂ and its series derivatives Li(Ni, Co, Mn)O₂ (NMC), as the main options for the cathode materials of Li-ion battery, has implemented industrial production because of their good comprehensive performance, including large capacity, good cycling and rate capability.¹⁻⁶ Thereinto, LiCoO₂ is the first commercialized cathode material, and still shares the biggest market due to the high volumetric energy-density and easy preparation.⁷ However, it also presents some drawbacks, such as relatively low practical capacity (around 140 mA h g⁻¹), high cost due to the rarity of Co source, and high toxicity of Co compared with Ni, Mn and Fe.^{8,9} So developing new cathode materials with high comprehensive performance attracted a lot of attention and efforts. Doping and replacement of Co with other TM elements becomes one of the successful strategies to tailor and enhance the electrochemical performance of cathode materials. Based on LiCoO₂, ternary Ni-Co-Mn system with different TM ratios, has been developed. Thereinto, Ni substitution is to improve the specific capacity with low cost, and Mn substitution is to enhance the structural stability of

layered oxide.¹⁰⁻¹² So, multiple TM substitution provides a vast potential to enhance the comprehensive electrochemical performance of layered materials.

With the advantage of tailoring properties by multiple TM substitution, it brings with another difficulty to implement uniform distribution of multiple metal elements in such a complicated polynary layered oxides system. In the traditional solid state method, mixing Li source and multiple TM sources by grinding or ball milling could not implement the great uniformity in precursors on nanometer or atomic scale. Thereinto, it is much more difficult to achieve the uniform distribution of TM elements with Li due to their much lower thermal diffusivities than Li.^{13,14} To solve this problem, a co-precipitation method was developed. It combines multiple TM elements into one compound, such as TM hydroxide,¹⁵⁻¹⁷ TM carbonate,¹⁸⁻²⁰ or TM oxalates,²¹ to implement the uniformity of TM elemental distribution, and then to mix it with Li-source to get layered oxides through high temperature calcination.

Inspired by the co-precipitation method, the best strategy to implement the uniform distribution of all metal elements is to combine all the involving metal elements (including Li and TM) in one single compound with correct ratios. This method is called as single molecular precursor method. Taking layered oxides LiTMO₂ as an example, it requires an appropriate ligand to combine Li and TM into one compound with Li/TM ratio as 1. Till now, there are only five cases to report the synthesis of cathode materials through single molecular precursor method by Dikarev group and Schneider group. Two of them are the synthesis of layered LiCoO₂.^{22,23} The other three are the synthesis of spinel LiMn₂O₄ and layered LiFeO₂.²⁴⁻²⁶ As we know, the synthesis of polynary layered oxides involving multiple TM cations, and their electrochemical performance through single molecular precursor method has never been demonstrated before. In addition, various organic ligands provide more choices than the limited inorganic precipitant (such as OH⁻ and CO₃²⁻), which might be beneficial to the co-precipitation efficiency of multiple metal cations.^{27,28}

In this work, a carbonyl-bridged single molecular precursor LiTM(acac)₃ (TM = Ni/Co/Mn, acac=acetylacetonate) featured 1D chain structure, was designed and applied to achieve the layered oxide cathode materials LiTMO₂ (TM=Ni/Co/Mn) here. Acac as carbonyl-rich ligand was chose to implement precise control of metal element compositions in single molecular precursors to lead to the correct compositions and great uniformity in the final products. As representatives, layered oxides, LiCoO₂, LiNi_{0.8}Co_{0.2}O₂ and LiNi_{0.5}Mn_{0.3}Co_{0.2}O₂

School of Advanced Materials, Peking University, Peking University Shenzhen Graduate School, Shenzhen 518055, China. E-mail: zhangmj@pkusz.edu.cn, panfeng@pkusz.edu.cn

Electronic Supplementary Information (ESI) available. See DOI: 10.1039/x0xx00000x

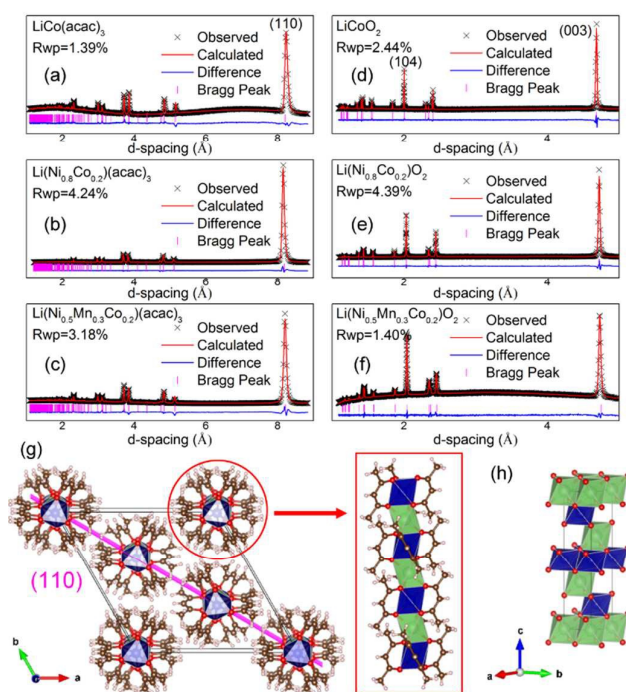


Fig. 1 Experimental XRD patterns of $\text{LiCo}(\text{acac})_3$ (a), $\text{Li}(\text{Ni}_{0.8}\text{Co}_{0.2})(\text{acac})_3$ (b) and $\text{Li}(\text{Ni}_{0.5}\text{Mn}_{0.3}\text{Co}_{0.2})(\text{acac})_3$ (c); experimental XRD patterns of LiCoO_2 (d), $\text{Li}(\text{Ni}_{0.8}\text{Co}_{0.2})\text{O}_2$ (e) and $\text{Li}(\text{Ni}_{0.5}\text{Mn}_{0.3}\text{Co}_{0.2})\text{O}_2$ (f); representative structural sketch maps of $\text{LiCo}(\text{acac})_3$ (g) and LiCoO_2 (h).

were successfully prepared through their single molecular precursors ($\text{LiCo}(\text{acac})_3$, $\text{LiNi}_{0.8}\text{Co}_{0.2}(\text{acac})_3$ and $\text{LiNi}_{0.5}\text{Mn}_{0.3}\text{Co}_{0.2}(\text{acac})_3$), respectively. They all exhibited good electrochemical performance due to the unique morphology and the great uniformity of elemental distribution.

The single molecular precursors were synthesized by the solution reflux method (details in ESI). As shown in Fig. S2, $\text{LiCo}(\text{acac})_3$, $\text{Li}(\text{Ni}_{0.8}\text{Co}_{0.2})(\text{acac})_3$ and $\text{Li}(\text{Ni}_{0.5}\text{Mn}_{0.3}\text{Co}_{0.2})(\text{acac})_3$ presented pink, lavender and light grey colors, respectively, with different TM compositions. The powder X-ray diffraction (XRD) pattern of $\text{LiCo}(\text{acac})_3$ was illustrated in Fig. 1a, which was consistent with the previous report.¹ The patterns of $\text{LiNi}_{0.8}\text{Co}_{0.2}(\text{acac})_3$ and $\text{LiNi}_{0.5}\text{Mn}_{0.3}\text{Co}_{0.2}(\text{acac})_3$ (Fig. 1b-c) were similar with that of $\text{LiCo}(\text{acac})_3$, which indicated that they all crystallized in a same space group ($R\bar{3}c$). The ICP-AES results (Table S1) indicated that the elemental compositions of Li and transition metals (TMs) were precisely controlled in the individual compound as designed. About 1% Li loss was observed after calcination. Their crystal structure was illustrated in Figure 1g. As we can see, it was constructed by a lot of parallel-aligned 1D chains along the c axis, which were consisted by the alternately-connected LiO_6 and TMO_6 octahedra within a face-sharing mode. Thereinto, each TMO_6 octahedron was composed by a TM cation chelated with three acac molecules, and one LiO_6 octahedron was composed by a Li ion bridged by six acac molecules. As shown in Figure 1h, the LiO_6 and TMO_6 octahedra are the basic structural units to produce the layered oxides LiTMO_2 .

To study the effect of TM compositions on the crystal structure, Rietveld refinements were performed for the three XRD patterns by using the reported $\text{LiCo}(\text{acac})_3$ structure as the initial model structure, and the relevant crystallographic parameters were deposited in Table S2 and Figure S2. As shown in Figure S2a, the unit cell parameters, a and c, firstly decreased with 80% Co(II) substitution with Ni (II), then

increased with further 30% Ni(II) substitution with Mn (II). On the other hand, this unique structure reflected that the organic ligand (acac) presented a much higher flexibility than the inorganic anions, OH^- and CO_3^{2-} , which could accommodate a much larger variation of metal-O bond lengths and long angles by the deformation of organic ligands. So it is the in-depth reason why the organic ligand could combine Li ions and various TM cations into one crystal framework. This character also allowed other metal cations to enter into the framework, thereby provide a great potential for various elemental doping.

The corresponding layered oxides LiCoO_2 , $\text{LiNi}_{0.8}\text{Co}_{0.2}\text{O}_2$ and $\text{LiNi}_{0.5}\text{Mn}_{0.3}\text{Co}_{0.2}\text{O}_2$ were prepared by calcining the corresponding precursors under preliminarily optimized conditions. Their structures were measured by powder X-ray diffraction (Fig. 1d-f). All diffraction peaks can be indexed to hexagonal LiCoO_2 ($R\bar{3}m$) with a layered structure (JCPDS no. 75-0532), revealing high phase purity for them. The (003) and (104) peaks of $\text{LiNi}_{0.8}\text{Co}_{0.2}\text{O}_2$ and $\text{LiNi}_{0.5}\text{Mn}_{0.3}\text{Co}_{0.2}\text{O}_2$ shifted to high d-spacing direction than LiCoO_2 , indicating larger lattice parameters after Ni and Mn substitution. Integrated intensity ratio of (003) to (104) peaks (denoted as $I(003)/I(104)$) was usually adopted to roughly evaluate the cationic disordering in layered structure.² Herein, high $I(003)/I(104)$ values for LiCoO_2 and $\text{LiNi}_{0.8}\text{Co}_{0.2}\text{O}_2$ (1.35, and 1.22, respectively), implied much less Li/Ni disordering in their layered structure, which hinted good electrochemical performance for them. Rietveld refinements were also performed for these three XRD patterns, and the relevant crystallographic parameters were deposited in Table S3 and Figure S2. As shown in Figure S2b, the lattice parameters, a and c, increased with the Ni and Mn substitution, which is consistent with the previous report.¹² The occupancy of Ni at 3b site (denoted as Ni(3b)) was another important indicator to show the Li/Ni disordering. Now the low Ni(3b) value (0.0394) in Table S3 also predicted good electrochemical performance for $\text{LiNi}_{0.8}\text{Co}_{0.2}\text{O}_2$.

The morphology of precursors and corresponding layered oxides were investigated by SEM characterization. As shown in Fig. 2, all the precursors presented prism-like shape, with length about 10-20 μm and width about 2-4 μm . This morphology was consistent with their hexagonal crystal structure shown in Fig. 1g, because the crystals preferred to grow up along the c axis by extending the 1D chain. The layered LiCoO_2 could be obtained by very low temperature, 450 $^\circ\text{C}$ (Fig. S6) with particle size around 200 nm (Fig. S7). When calcined at higher temperature (850 $^\circ\text{C}$), the nanocrystals merged and grew significantly by about ten times. As shown in Fig. 3a, a thick plate was composed by small particles with size around 2 μm . The high-magnification SEM images in Fig. 3b showed the micrometer pillar shape with surface-exposed layered texture, a unique morphology for LiCoO_2 that has never been reported before. These surface-exposed layered textures could be assigned to (003) crystal plane according to its layered structure shown in Fig. 1h, which might be beneficial to Li^+ fast de/intercalation to enhance the rate capability. After sintering $\text{LiNi}_{0.8}\text{Co}_{0.2}(\text{acac})_3$ at 800 $^\circ\text{C}$ for 8 h, $\text{LiNi}_{0.8}\text{Co}_{0.2}\text{O}_2$ presented a 3D network framework composed with small particles (Fig. 3c) with the size about 500 nm (Fig. 3d). As shown in Fig. 3e-f, $\text{LiNi}_{0.5}\text{Mn}_{0.3}\text{Co}_{0.2}\text{O}_2$ showed a similar 3D network morphology constructed with much smaller particles. The EDX elemental mappings were performed for three materials to study the elemental distribution of transition metals. Fig. S9 displayed that Ni, Mn and Co distributed uniformly in these samples. In addition, the chemical compositions of three single molecular precursors and the corresponding layered oxides were measured by ICP-AES

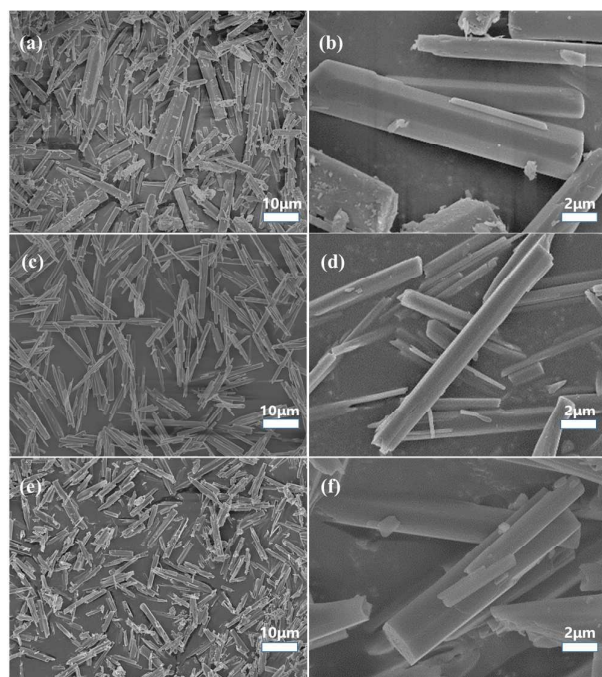


Fig. 2 Low magnification (a) and high magnification (b) SEM images of LiCoO_2 ; Low magnification (c) and High magnification (d) SEM images of $\text{LiNi}_{0.8}\text{Co}_{0.2}\text{O}_2$; Low magnification (e) and High magnification (f) SEM images of $\text{LiNi}_{0.5}\text{Mn}_{0.3}\text{Co}_{0.2}\text{O}_2$.

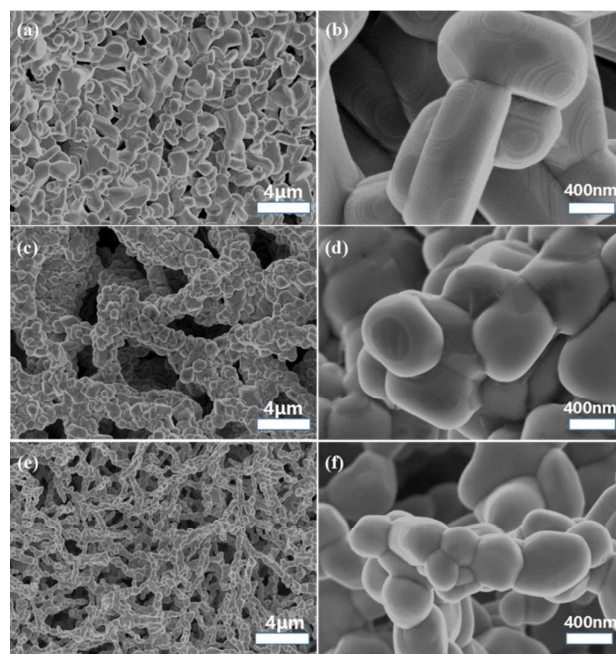


Fig. 3 Low magnification (a) and high magnification (b) SEM images of LiCoO_2 ; Low magnification (c) and High magnification (d) SEM images of $\text{LiNi}_{0.8}\text{Co}_{0.2}\text{O}_2$; Low magnification (e) and High magnification (f) SEM images of $\text{LiNi}_{0.5}\text{Mn}_{0.3}\text{Co}_{0.2}\text{O}_2$.

(Table S1). It is clear that, the molar ratios of metal elements including Li, Ni, Co, and Mn were consistent with the pre-designed. After calcination, the molar ratios of metal elements nearly kept constant. It further proved that the elemental composition could be precisely controlled by this single molecular precursor method.

Finally, LiCoO_2 , $\text{LiNi}_{0.8}\text{Co}_{0.2}\text{O}_2$ and $\text{LiNi}_{0.5}\text{Mn}_{0.3}\text{Co}_{0.2}\text{O}_2$ were assembled into half cells to test their electrode performance (see Experimental Section in the ESI†). Fig. 4a showed the charge and discharge profiles of the first two cycles with a current density of 18 mA g^{-1} between 2.7 and 4.4V for LiCoO_2 . 1st charge and discharge capacities were 180.9 and $171.3 \text{ mA h g}^{-1}$, and the capacities for 2nd cycle were 170.5 and $170.1 \text{ mA h g}^{-1}$, respectively. The coulombic efficiencies for the 1st and 2nd cycle were calculated to be 94.6% and 99.7%, respectively. So large capacities were superior to most of LiCoO_2 samples prepared by traditional solid state method and other methods.^{29–32} The small capacity loss during the 1st cycle could be ascribed to the irreversible loss of Li ions caused by the formation of SEI films. Fig. 4b exhibits the electrode capacities tested at the current densities increasing from 18 to 36, 90, 180, 360, 900, and 1800 mA g^{-1} , and five cycles were performed at each rate. The corresponding discharge capacities could reach 170, 165, 160, 155, 146, 128, and 86 mA h g^{-1} , respectively. The reversible capacity recovered to 163 mA h g^{-1} when the current density was brought back to 18 mA g^{-1} . Fig. 4c further illustrates the cycling performance of LiCoO_2 with a current density of 180 mA g^{-1} at 25°C , which can retain a reversible capacity of $136.6 \text{ mA h g}^{-1}$ with capacity retention of 88.7% after 50 cycles.

Similarly, Fig. 4d showed the charge and discharge profile of $\text{LiNi}_{0.8}\text{Co}_{0.2}\text{O}_2$ with a current density of 18 mA g^{-1} . It presented the charge and discharge capacities of 193.8 and $181.13 \text{ mA h g}^{-1}$ for the 1st cycle, 183.4 and $180.9 \text{ mA h g}^{-1}$ for the 2nd cycle. Higher capacities and lower voltage plateaus was observed by comparing it with pure LiCoO_2 after Ni

substitution, which was consistent with previous reports.^{33–35} The coulombic efficiencies were also very high, 93.4% and 98.6% for the 1st and 2nd cycle, respectively. Fig. 4e presented an excellent rate capability, which was similar with pure LiCoO_2 . Fig. 4f further illustrates the cycling performance of $\text{LiNi}_{0.8}\text{Co}_{0.2}\text{O}_2$. The capacity retention was 81.5% after 50 cycles, which was lower than pure LiCoO_2 . It might be due to high Ni reactivity and structural reconstruction on the particle surface for high Ni layered oxides.³⁶ These excellent cycling and rate performance could compare to or superior to that of $\text{LiNi}_{0.8}\text{Co}_{0.2}\text{O}_2$ prepared by traditional solid state method and other methods.^{37–39} Fig. 4g–i showed the charge and discharge profiles, rate and cycling performance for $\text{LiNi}_{0.5}\text{Mn}_{0.3}\text{Co}_{0.2}\text{O}_2$, respectively. It was clear that the charge/discharge capacities decreased in comparison with LiCoO_2 and $\text{LiNi}_{0.8}\text{Co}_{0.2}\text{O}_2$ after Mn substitution. The rate performance was also deteriorated after Mn substitution. Nevertheless, its cycling performance shown in Fig. 4i was greatly increased due to Mn replacement. A super high capacity retention of 98.5% was obtained after 50 cycles. In one word, Mn substitution decreased the capacity and rate capability, but increased the cycling stability. This result is in accord with Mn role in layered oxide, i.e., improving the structural stability.¹¹ In addition, the low capacity and poor rate capability might be due to high Li/Ni mixing and small grain size shown in Table S3.

In summary, multiple layered oxides LiTMO_2 , including LiCoO_2 , $\text{LiNi}_{0.8}\text{Co}_{0.2}\text{O}_2$ and $\text{LiNi}_{0.5}\text{Mn}_{0.3}\text{Co}_{0.2}\text{O}_2$, were prepared by the thermal decomposition of a versatile precursor $\text{LiTM}(\text{acac})_3$. They not only present unique morphology with great uniformity of element distribution, but also exhibit good electrochemical performance. It provides a unique and valuable approach to prepare high performance electrode materials for LIBs. More layered cathode materials, such as NCA, NCM with other TM ratios, even including layered sodium ion materials, are expected to be prepared by this method.

COMMUNICATION

Journal Name

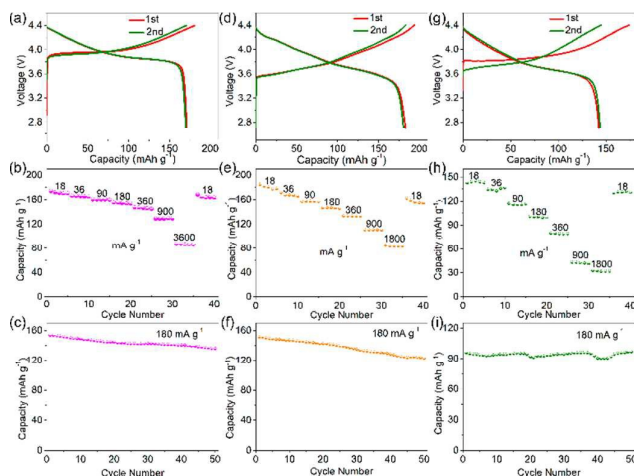


Fig. 4 Electrochemical performance of LiCoO_2 , $\text{LiNi}_{0.8}\text{Co}_{0.2}\text{O}_2$ and $\text{LiNi}_{0.5}\text{Mn}_{0.3}\text{Co}_{0.2}\text{O}_2$. Charge and discharge profile at selected cycles with a current density of 18 mA g^{-1} for LiCoO_2 (a), $\text{LiNi}_{0.8}\text{Co}_{0.2}\text{O}_2$ (d) and $\text{LiNi}_{0.5}\text{Mn}_{0.3}\text{Co}_{0.2}\text{O}_2$ (g); rate performance at various current densities for LiCoO_2 (b), $\text{LiNi}_{0.8}\text{Co}_{0.2}\text{O}_2$ (e) and $\text{LiNi}_{0.5}\text{Mn}_{0.3}\text{Co}_{0.2}\text{O}_2$ (h); and cycling performance with a current density of 180 mA g^{-1} at 25°C for LiCoO_2 (c), $\text{LiNi}_{0.8}\text{Co}_{0.2}\text{O}_2$ (f) and $\text{LiNi}_{0.5}\text{Mn}_{0.3}\text{Co}_{0.2}\text{O}_2$ (i).

Conflicts of interest

There are no conflicts to declare.

Acknowledgements

This work was supported by the peacock plan (KYPT20141016105435850), the Guangdong innovative team program (2013N080), Chinese postdoctoral science foundation (2015M570882, 2015M570894), Shenzhen Science and Technology Research Grant (JCYJ20151015162256516, JCYJ20150729111733470), the U. S. Department of Energy (DOE) Office of Energy Efficiency and Renewable Energy under the Advanced Battery Materials Research (BMR) program (DE-SC0012704).

Notes and references

- N. A. Chernova, G. M. Nolis, F. O. Omenya, H. Zhou, Z. Li and M. S. Whittingham, *J. Mater. Chem.*, 2011, 21, 9865-9875.
- M. M. Thackeray, C. Wolverton and E. D. Isaacs, *Energy Environ. Sci.*, 2012, 5, 7854-7863.
- N. Nitta, F. X. Wu, J. T. Lee and G. Yushin, *Mater. Today*, 2015, 18, 252-264.
- M. D. Radin, S. Hy, M. Sina, C. Fang, H. Liu, J. Vinkeviciute, M. Zhang, M. S. Whittingham, Y. S. Meng and A. Van der Ven, *Adv. Energy Mater.*, 2017, 7, 1602888.
- G. Crabtree, E. Kocs and L. Trahey, *MRS Bull.*, 2015, 40, 1067-1078.
- D. Andre, S. J. Kim, P. Lamp, S. F. Lux, F. Maglia, O. Paschos and B. Stiasny, *J. Mater. Chem. A*, 2015, 3, 6709-6732.
- K. Mizushima, P. C. Jones, P. J. Wiseman and J. B. Goodenough, *Mater. Res. Bull.*, 1980, 15, 783-789.
- E. M. Erickson, C. Ghanty and D. Aurbach, *J. Phys. Chem. Lett.*, 2014, 5, 3313-3324.
- B. L. Ellis, K. T. Lee and L. F. Nazar, *Chem. Mater.*, 2010, 22, 691-714.

- W. Liu, P. Oh, X. Liu, M. J. Lee, W. Cho, S. Chae, Y. Kim and J. Cho, *Angew. Chem. Int. Ed.*, 2015, 54, 4440-4457.
- A. Manthiram, J. C. Knight, S. T. Myung, S. M. Oh and Y. K. Sun, *Adv. Energy Mater.*, 2016, 6, 1501010.
- J. M. Zheng, W. H. Kan and A. Manthiram, *ACS Appl. Mater. Interfaces*, 2015, 7, 6926-6934.
- J. Li, R. Doig, H. S. Liu, G. Botton and J. R. Dahn, *J. Electrochem. Soc.*, 2016, 163, A2841-A2848.
- J. Li, R. Shunmugasundaram, R. Doig and J. R. Dahn, *Chem. Mater.*, 2016, 28, 162-171.
- X. M. Zhao, F. Zhou and J. R. Dahn, *J. Electrochem. Soc.*, 2008, 155, A642-A647.
- Y. K. Sun, Y. C. Bae and S. T. Myung, *J. Appl. Electrochem.*, 2005, 35, 151-156.
- M. E. Spahr, P. Novak, B. Schnyder, O. Haas and R. Nesper, *J. Electrochem. Soc.*, 1998, 145, 1113-1121.
- L. Xu, P. Y. Hou, Y. T. Zhang, H. Z. Zhang, D. W. Song, X. X. Shi, X. Q. Wang and L. Q. Zhang, *J. Mater. Chem. A*, 2015, 3, 21219-21226.
- F. L. Liu, S. Zhang, C. Deng, Q. Wu, M. Zhang, F. L. Meng, H. Gao and Y. H. Sun, *J. Electrochem. Soc.*, 2012, 159, A1591-A1597.
- T. H. Cho, S. M. Park and M. Yoshio, *Chem. Lett.*, 2004, 33, 704-705.
- J. W. Kou, Z. Wang, L. Y. Bao, Y. F. Su, Y. Hu, L. Chen, S. Y. Xu, F. Chen, R. J. Chen, F. C. Sun and F. Wu, *Acta Phys.-Chim. Sin.*, 2016, 32, 717-722.
- Z. Wei, H. X. Han, A. S. Filatov and E. V. Dikarev, *Chem. Sci.*, 2014, 5, 813-818.
- J. Khanderi and J. J. Schneider, *Eur. J. Inorg. Chem.*, 2010, 2010, 4591-4594.
- A. Navulla, L. Huynh, Z. Wei, A. S. Filatov and E. V. Dikarev, *J. Am. Chem. Soc.*, 2012, 134, 5762-5765.
- H. X. Han, Z. Wei, M. C. Barry, A. S. Filatov and E. V. Dikarev, *Dalton Trans.*, 2017, 46, 5644-5649.
- J. Khanderi and J. J. Schneider, *Inorg. Chim. Acta*, 2011, 370, 254-259.
- A. Bommel and J. R. Dahn, *Chem. Mater.*, 2009, 21, 1500-1503.
- H. Dong and G. M. Koenig Jr, *J. Mater. Chem. A*, 2017, 5, 13785-13789.
- Z. G. Wang, Z. X. Wang, W. J. Peng, H. J. Guo, X. H. Li, J. X. Wang and A. Qi, *Ionics*, 2014, 20, 1525-1534.
- Q. Cao, H. P. Zhang, G. J. Wang, Q. Xia, Y. P. Wu and H. Q. Wu, *Electrochem. Commun.*, 2007, 9, 1228-1232.
- B. Huang, Y. I. Jang, Y. M. Chiang and D. R. Sadoway, *J. Appl. Electrochem.*, 1998, 28, 1365-1369.
- Y. Takahashi, S. Tode, A. Kinoshita, H. Fujimoto, I. Nakane and S. Fujitani, *J. Electrochem. Soc.*, 2008, 155, A537-A541.
- X. X. Li, F. Y. Cheng, B. Guo and J. Chen, *J. Phys. Chem. B*, 2005, 109, 14017-14024.
- H. J. Kweon, S. S. Kim, G. B. Kim and D. G. Park, *J. Mater. Sci. Lett.*, 1998, 17, 1697-1701.
- V. Etacheri, R. Marom, R. Elazari, G. Salitra and D. Aurbach, *Energy Environ. Sci.*, 2011, 4, 3243-3262.
- F. Lin, I. M. Markus, D. Nordlund, T. C. Weng, M. D. Asta, H. L. L. Xin and M. M. Doeff, *Nat. Commun.*, 2014, 5, 3529.
- C. Zhu, C. Yang, W. D. Yang, M. S. Wu, H. M. Ysai, C. Y. Hsieh and H. L. Fang, *J. Appl. Electrochem.*, 2010, 40, 1665-1670.
- L. F. Xiao, Y. Y. Yang, Y. Q. Zhao, X. P. Ai, H. X. Yang and Y. L. Cao, *Electrochim. Acta*, 2008, 53, 3007-3012.
- M. Sathya, K. Hemalatha, K. Ramesha, A. K. Shukla and A. S. Prakash, *Bull. Mater. Sci.*, 2011, 34, 1693-1698.

Table of contents

A versatile single molecular precursor $\text{LiTM}(\text{acac})_3$ featured 1D chain structure, was developed to achieve the layered oxides LiTMO_2 (TM=Ni/Co/Mn, NMC) for Li-ion batteries.

